Theoretical and Applied Climatology (2023) 153:73–86
https://doi.org/10.1007/s00704-023-04517-x

ORIGINAL PAPER

Role of north Indian Ocean on the lightning flash rate of the Indian land region

P. G. Nisha[1] · T. S. Pranesha[1] · M. Ravichandran[2]

Received: 31 January 2022 / Accepted: 29 May 2023 / Published online: 5 June 2023
© The Author(s), under exclusive licence to Springer-Verlag GmbH Austria, part of Springer Nature 2023

Abstract

Thunderstorm activity and lightning have been extensively studied due to their link with severe weather phenomenon. Intense thunderstorms have higher lightning flash rates (LFR), and this study investigates the causative mechanisms of such higher LFR over the Indian land region. Higher LFR occurs over India during pre-monsoon, monsoon and post-monsoon seasons. The results show that flash rates over the Indian land region depend on local heating and moisture availability enhanced by the heat content and moisture advection from the surrounding sea. The increase in the heat content of the Arabian Sea and Bay of Bengal during the pre-monsoon, monsoon and post-monsoon periods causes deep convection over the Seas to a higher altitude, which is then advected into the land by the winds. This increases the heat and turbulent heat flux over the land, and hence fuelling the thunderstorms, subsequently altering the flash rate. Multiple regression and correlation analysis show that the heat content and moisture advection from the Arabian Sea and Bay of Bengal have a major influence on the regions with higher LFR.

Keywords Lightning · Indian Ocean · Turbulent heat flux · Heat content · Moisture advection

1 Introduction

Globally, lightning over the land area is higher than that over the oceans (Williams 2005; Price 2009), with the highest percentage found over the tropical belt, especially Southeast Asia, Africa and South America (Turman and Edgar 1982; Price 2009; Cecil et al. 2014). Chate et al. (2016) observed that the annual lightning flash counts are higher over Indian land than over Indo-Gangetic Plain (IGP) and Indian seas. The study also suggested that the turbulent heat flux represents the best parameter for describing lightning activity over IGP and Indian land.

Thunderstorms are 'convective' in nature and these deep moist convective storms, represent local-scale (2–20 km) circulations driven under conditionally unstable environments by conversion of potential buoyant energy to the kinetic energy within the updraft. Surface heat flux is the key factor in converting convective available potential energy (CAPE) into kinetic energy of updraft in the deep convective systems (Yuan and Qie 2005; Sátori et al. 2009). Other than surface heating, dynamical forcing of vertical motion stands as another important parameter for the development of thunderstorms. CAPE represents the total excess buoyancy indicating that an air parcel would be much warmer than its surrounding environment. Over regions of the updraft, CAPE also relates to the vertical velocity of the air and hence higher values indicate greater potential for severe weather. A strong correlation of lightning activity with rainfall and CAPE is observed over tropical centres in South Asia (Yoshida et al. 2009; Murugavel et al. 2014; Saha et al. 2017; Tinmaker et al. 2015, 2019). Previous studies (Manohar and Kesarkar 2004; Kandalgaonkar et al. 2005; Tyagi 2007; Tinmaker et al. 2010a, b, 2019; Penki and Kamra 2013; Murugavel et al. 2014; Kamra and Ramesh Kumar 2021; Unnikrishnan et al. 2021; Sarkar et al. 2022) have reported spatial variations of thunderstorm activity over the Indian region. The highest frequency has been observed over Assam and Sub Himalayan West Bengal in the east and Jammu region in the north, whereas the lowest frequency is observed over the Ladakh region. Over peninsular India, the highest thunderstorm activity is observed over Kerala.

✉ P. G. Nisha
nishapg@gmail.com

[1] Department of Physics, B.M.S. College of Engineering, Bull Temple Road, Bengaluru, Karnataka 560019, India

[2] National Centre for Polar and Ocean Research (NCPOR), Ministry of Earth Sciences, Headland Sada, Vasco-da-Gama, Goa 403804, India

Lightning activity is predominant over the Indian region during the pre-monsoon and the post-monsoon season which are of utmost importance as they contribute significantly to the annual total rainfall over the Indian region (Manohar et al. 1999). The maximum lightning activity was reported to be occurring in May with a diurnal maximum during afternoon/evening time duration (Kandalgaonkar et al. 2003; Sarkar et al. 2022). Circulation patterns within the planetary boundary layer also play a role in the development of storm conditions. The evolution of the convective system and the energy budget during its life cycle also depends on the horizontal advection of moisture by the large-scale circulations.

A major part of the heat stored in the ocean is released to the atmosphere through turbulent surface heat fluxes such as latent heat flux (LHF) and sensible heat flux (SHF) (Large and Pond 1982). LHF is the transfer of heat due to water phase changes, such as evaporation or condensation between the surface and atmosphere through the effects of turbulent air motion. SHF is governed by the difference in temperature between the surface and the overlying atmosphere, wind speed and surface roughness. Nisha et al. (2012) have reported the variations of LHF and moisture with sea surface temperature (SST) over the Indian Ocean. Over the ocean, an increase in SST would increase convection which in turn can cause higher lightning activity associated with convective storms (Kandalgaonkar et al. 2002; Tinmaker et al. 2010a, b, 2014). Along with SST, the upper ocean heat content is now considered an important parameter for the development and intensification of convective systems like tropical cyclones (Mainelli et al. 2008; Pun et al. 2013; Emanuel 2015; Mawren and Reason 2017; Vidya et al. 2021).

The existing literature review suggests that no major work has been done to study the inter-relationship of moisture advection and ocean heat content with the surface and convective systems like thunderstorms over the land region. Both latent and sensible heat fluxes propagate energy through the atmosphere and are the major source of energy in driving wind and vertical motions. It is important to study the association of heat content and turbulent heat flux of the north Indian Ocean on the meteorological parameters over the Indian region which can reveal important air–sea interactions. In this study, we have reported the seasonal, monthly and interannual variations of lightning activity over the Indian land region and analysed the role of the north Indian Ocean on such variabilities.

2 Data and methods

2.1 Data used

Low-resolution monthly time series (LRMTS) lightning data from January 1996 to December 2013 of 2.5°×2.5° resolutions are used in this study. LRMTS of lightning flash rates (LFR, counts/km^2/day) involves data from both lightning imaging sensor (LIS) and optical transient detector (OTD) in a combined form for each month. OTD on the MicroLab-1 satellite and LIS on the Tropical Rainfall Measuring Mission (TRMM) satellite is a part of the National Aeronautics and Space Administration's (NASA) Earth Observing System (EOS) (Cecil et al. 2014). LIS detects lightning flashes with a resolution of 4 to 7 km over a large region (600×600 km^2) of the Earth's surface. OTD has a spatial resolution of 1300×1300 km^2 (about 1/300 of the total surface area of the Earth). OTD is a compact combination of optical and electronic sensors designed for observing and measuring lightning from space. The data of LFR are retrieved from https://ghrc.nsstc.nasa.gov/lightning/data/data_lis_otd-climatology.html.

The monthly data for turbulent heat fluxes like LHF and SHF, humidity, zonal and meridional components of wind velocity, and CAPE, required for the study, from January 1996 to December 2013 are used from ECMWF Re-Analysis 5 (ERA5) and are available at https://www.ecmwf.int/en/forecasts/datasets/reanalysis-datasets/era5, with a resolution of 0.25°×0.25°. ERA5 provides estimates of a large number of atmospheric, land and oceanic climate variables, based on 4D-Var data assimilation using Cycle 41r2 of the Integrated Forecasting System (IFS), which was operational at ECMWF in 2016 (Hersbach et al. 2020). LHF depends on wind and humidity whereas sensible heat flux depends on wind and temperature difference between surface and air. Turbulent heat flux gives an account of the transfer of energy between surface and atmosphere and is obtained by adding the LHF and SHF. CAPE marks the conditional instability in the atmosphere, where an ascending air parcel is warmer than the surroundings. It is used to assess the possibilities of the development of convection, which can lead to intense thunderstorms with associated heavy rainfall.

The monthly mean of ocean temperature and salinity data at a spatial resolution of 1°×1° with 42 levels in the vertical, from January 1996 to December 2013 are obtained from ECMWF Ocean Reanalysis System 4 (ORAS4) for computing heat content (Balmaseda et al. 2013). The data is available at http://www.ecmwf.int/products/forecasts/d/charts/oras4/reanalysis/ from 1958 to 2017.

The ocean reanalyses are the reconstruction of the ocean state, using ocean models forced by atmospheric forcing fluxes and also assimilated with ocean observations, both from in situ and satellites.

2.2 Methodology

Moisture advection is calculated using the below equation:

$$\frac{dq}{dt} = -\left[u\frac{dq}{dx} + v\frac{dq}{dy} + z\frac{dq}{dz}\right] \quad (1)$$

where, q is specific humidity, u, v and w are zonal, meridional and vertical wind velocity, respectively. In this study, only the horizontal moisture advection due to the zonal and meridional components of wind is considered.

The heat content is calculated using the equation:

$$\mathrm{HC} = \rho C_p \int_{h1}^{h2} T(z)\mathrm{d}z \tag{2}$$

where ρ is the density of the seawater, C_p is the specific heat capacity of the seawater at constant pressure, p; h_1 and h_2 are the depth range where the heat content is calculated, here surface to 100 m, and T is the seawater temperature. The parameters are analysed for four seasons namely pre-monsoon (March–May), monsoon (June–September), post-monsoon (October–November) and winter (December–February).

Multiple regression model is employed for the detailed analyses of dependency of LFR on moisture advection and heat content from Arabian Sea and Bay of Bengal. This statistical technique is used for modelling and analysing several variables by describing the relation between a dependent variable and several independent variable.

Y is a one-dimensional array of length i containing the dependent variable y_i. X is a two-dimensional array of size (i,n) where n is the number of independent variables:

$$y_i = b_0 + b_1 x_{i1} + b_2 x_{i2} + b_3 x_{i3} + \cdots + b_n x_{\mathrm{in}} \tag{3}$$

Equation (3) represents the least square regression line for multiple regression of n independent variables where, b_0 is the y-intercept (constant term), x_{in} is the nth independent variable and b_n is the coefficient of the nth independent variable. When all the independent variables $x_{i1}, x_{i2} \ldots \ldots x_{\mathrm{in}}$ are constant the predicted value of y_i is b_0. The predicted value of y_i changes by b_n for each one unit increase in x_{in}, keeping the other variables are constant.

The standardised regression coefficients 'b_{std}' are calculated from the partial regression coefficient b. 'b_{std}' represents the regression coefficient in units of standard deviation and can be directly compared with each other to determine the most effective independent variables.

$$b_{\mathrm{std}j} = b_j \times \frac{\sigma(X)}{\sigma(Y)} \tag{4}$$

where, $j = 1, 2 \ldots\ldots n$ and $\sigma(X)$, $\sigma(Y)$ are the standard deviation of X and Y, respectively.

3 Observations

Seasonal climatology computed from monthly data of LFR from 1996 to 2013 over the Indian region is shown in Fig. 1. LFR is prominent over three regions, viz North, Northeast and South peninsular region. During pre-monsoon, maximum flash rate is observed over northeast regions, and lesser intensity of lightning in the north and southern peninsular (Fig. 1a). The average flash rate of ~ 0.12 to 0.14 counts km^{-2} day^{-1} over the northeast, ~ 0.07 to 0.09 counts km^{-2} day^{-1} over the north and ~ 0.05 to 0.07 counts km^{-2} day^{-1} over the southern peninsular region is observed during this period. During monsoon, the north and north east region show a significant flash rate of ~ 0.1 to 0.14 counts km^{-2} day^{-1} and ~ 0.06 counts km^{-2} day^{-1} (Fig. 1b).

During post-monsoon, thunderstorm activity prevails over these regions but is observed to be comparatively less (Fig. 1c). LFR is observed to be negligible throughout the Indian region during winter (Fig. 1d). The areas with maximum LFR for further analysis are identified as the North region (NR; 28° N–36° N; 70° E–77° E); East region (ER; 22° N–26° N; 85° E–95° E) and South region (SR; 8° N–15° N; 75° E–80° E), as shown in Fig. 1d. To study the monthly variations of flash rates over the areas of maximum LFR, monthly climatology of the LFR for ER, SR and NR are computed (Fig. 2) using the data from 1996 to 2013. Over ER, flash rate increases and reaches a maximum during April and May, and then decreases sharply with the onset of monsoon until July (Fig. 2, black line). The rate of fall in flash rates is observed to be decreasing during August–September, after which the fall rate increases rapidly. A similar pattern of variation in flash rates is observed over SR, with comparatively less amplitude (Fig. 2, red line). For both regions, the maximum flash rate is seen during the pre-monsoon period. These higher flash rates are due to the higher local heating during the pre-monsoon which triggers convective activity, intensifying into thunderstorms (Manohar et al. 1999; Williams and Stanfill 2002; Williams et al. 2005; Tinmaker et al. 2010b). As monsoon sets in, the thermal heating reduces and the moisture-laden winds from the Arabian Sea tend to cool down the convective activity over the southern and then the eastern regions of India. During monsoon, due to the presence of clouds with the moderate updraft, the cloud electrification remains minimum, thus reducing the flash count over the SR region (Takahashi 1990; Manohar et al. 1999; Kandalgaonkar et al. 2008). Over SR, a secondary maximum is observed during the month of September–October similar to the ER region. During September, the cloud bases of the thunderstorms are at lower altitudes (Manohar and Kandalgaonkar 1995). These months mark the withdrawal phase of monsoon with less rainfall and clouds and more solar local heating. Moreover, with enough moisture availability to sustain the development of thunderstorms, these months mark a higher LFR (Tinmaker et al. 2010a, b). The high LFR during pre-monsoon and post-monsoon may also be due to the influence of

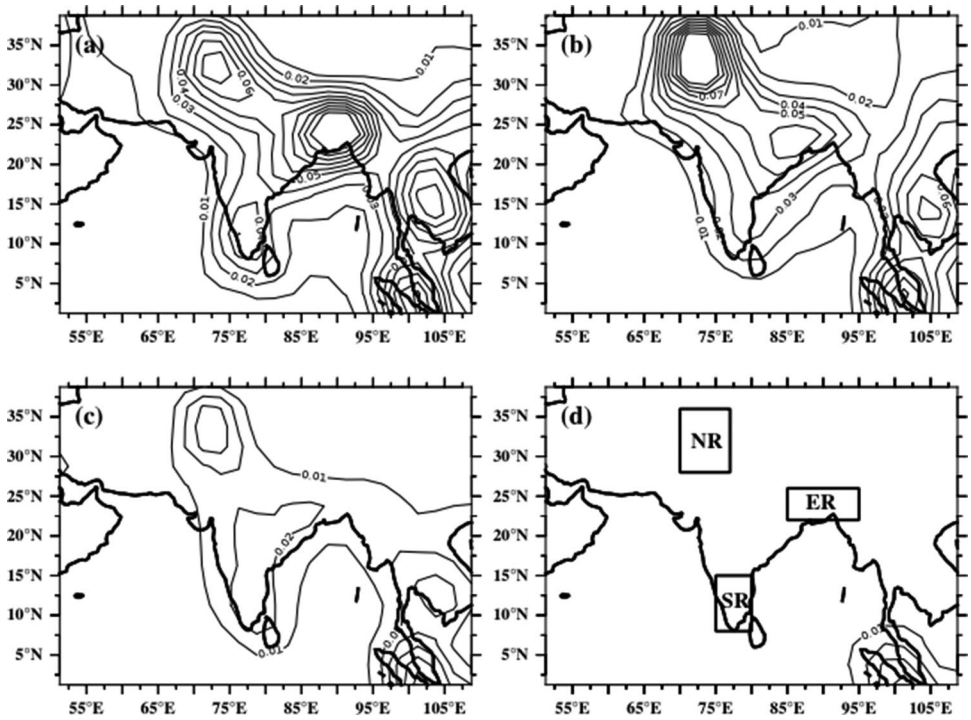

Fig. 1 Climatological spatial variations of LFR (counts km^{-2} $day.^{-1}$) during four seasons, **a** pre-monsoon, **b** monsoon, **c** post-monsoon and **d** winter during 1996 to 2013. Area of study shown in **d** East 22° N–26° N; 85° E–95° E (ER), South 8° N–15° N; 75° E–80° E (SR) and North 28° N–36° N; 70° E–77° E (NR)

the cyclonic activity during these seasons in the Arabian Sea and Bay of Bengal.

Over NR, heating prevails during June–July, because of the delay in the arrival of monsoon winds. NR region remains comparatively dry to the coastal ER and SR regions. Hence, flash rates show high values during June-July and decrease thereafter (Fig. 2, blue line) with the onset of monsoon clouds over this region. Thus, the peak LFR shows a shift towards June–July in NR, compared to pre-monsoon peaks in ER and SR regions. This shift in the LFR peak may be due to the northward shift in deep convective activity which prevails over east coast of India during pre-monsoon, to the western Himalayan foothills during monsoon (Romatschke et al. 2010). LFR over NR shows a rapid fall after July as the monsoon winds shadow the convective activity, cooling down the temperatures.

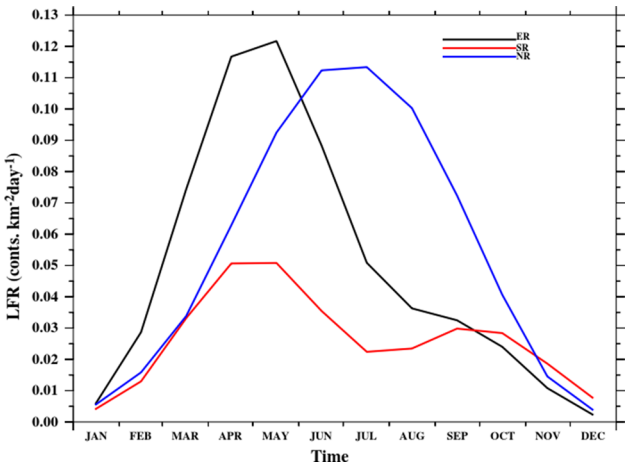

Fig. 2 Monthly climatology of LFR over ER (black), SR (red) and NR (blue) regions during 1996 to 2013

Average flash rates throughout the year are high over ER and NR, whereas low in SR. The two prominent peaks observed in SR with primary maxima during April–May is also observed in ER but with less prominent secondary peak during September. This shows semi-annual variability of flash rates. Only one major peak appears for NR region with maxima during June–July demonstrating annual variability. Such annual variabilities over regions with elevated orography and semi-annual variabilities in flash rates over the coastal and non-elevated regions were also observed by Kamra and Ramesh Kumar 2021.

3.1 Effect of local heating and turbulent heat flux on LFR

It is well known that the occurrence of thunderstorms mainly depends on local heating. Figure 3 shows the climatological monthly mean of CAPE and turbulent heat flux for ER, SR and NR during the period 1996 to 2013.

Over ER, CAPE variations show a pattern similar to that of the flash rates (Fig. 2, black line) with a maximum of ~ 1300 Jkg^{-1} during April–May and a secondary peak during September (Fig. 3a, black line). SR also shows two peaks for CAPE, one during the pre-monsoon period and the other during September–October (Fig. 3b, black line).

The maximum amplitude for CAPE is observed during pre-monsoon reaching more than 1000 Jkg^{-1}. For NR, the curves of CAPE show a similar pattern as that of the flash rate curve (Fig. 2, blue line), but with a shift of one month (Fig. 3c, black line) when compared to the other regions. LFR attains its maximum value during June–July, whereas for CAPE, the maxima are during July–August. Both the parameters show only one peak for NR, unlike the other two regions. From these figures, it is evident that the flash rates are not only dependent on CAPE but also influenced by other parameters.

One such parameter that can affect thunderstorm formation is the turbulent heat fluxes (Toumi and Qie 2004; Chate et al. 2016; Tinmaker et al. 2019; Sreenath et al. 2021; Gautam et al. 2022).

Turbulent fluxes are mainly based on land surface properties. The surface latent heat flux is maximum over land with more vegetation cover or wetlands, whereas surface sensible heat flux shows its maximum over dry land mass. Continental surfaces gets heated faster and are more unstable to vertical air motions leading to deep convection, exhibiting more sensible heat flux compared to the sea.

Figure 3 also shows the monthly mean of turbulent heat flux (red line) throughout the year, for ER, SR and NR. Over ER, the turbulent heat flux variations show two peaks, the first and prominent one during April–May with the highest value of ~ 110 Wm^{-2}, and a secondary peak at ~ 90 Wm^{-2} during August–September (Fig. 3a, red line). From May–June–July, the turbulent flux is observed to be comparatively less, which is similar to the pattern observed in LFR over the same region. Over SR, the turbulent flux shows two peaks during May and September with a heat flux of 100–115 W m^{-2} (Fig. 3b, red line). The monthly variations of turbulent heat flux show a one-to-one similarity with the flash rate curve. Variations of heat flux over NR are observed to be different from the other two regions (Fig. 3c, red line) with a maximum amplitude of ~ 100 W m^{-2} during June and July, and thereafter decreasing until December. LFR variations are slightly steeper over both sides of the maxima than that of turbulent heat flux variations (Fig. 2. blue line).

The above results show that the LFR increases from April as the convection sets in over these regions. Over SR, as the monsoon reaches during early June, convection gets suppressed, which causes the flash rates to drop down from June onwards. Over ER and NR, due to the delay in the arrival of monsoon, the turbulent heat flux and flash rates start decreasing from July onwards. Hence, both CAPE and turbulent heat fluxes are major influences for the development of thunderstorms in the Indian land mass. Furthermore, we investigate the role of surrounding seas over LFR over the Indian region in the subsequent sections.

3.2 Role of ocean heat content and moisture advection

Tinmaker et al. (2010a, b) have shown the importance of the SST of the Arabian Sea and Bay of Bengal on the

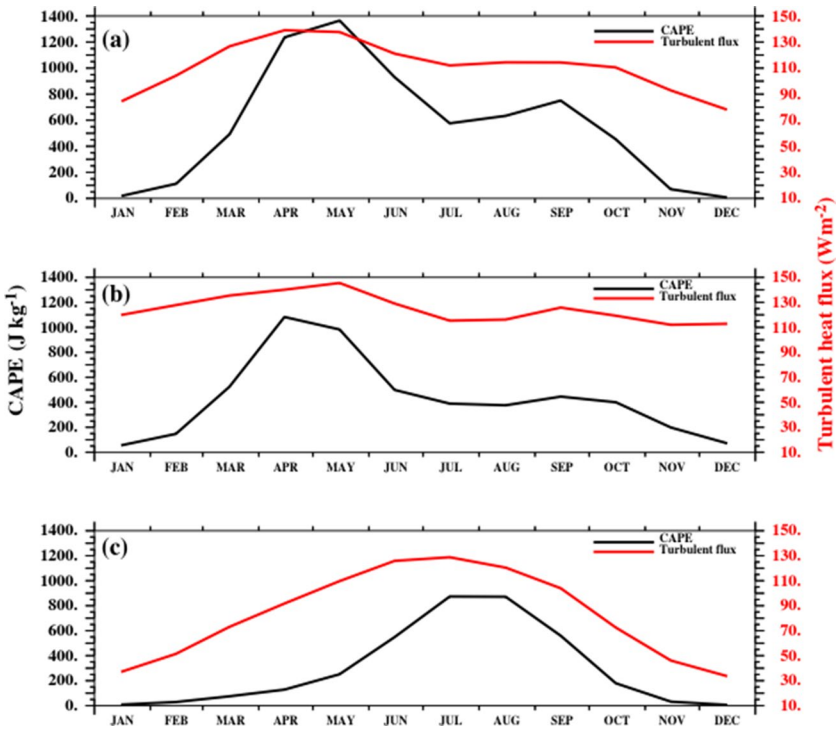

Fig. 3 Monthly mean of CAPE (black) and turbulent heat flux (red) over **a** ER, **b** SR and **c** NR during 1996 to 2013

development of thunderstorms over the Indian south peninsular region. In this section, we analyse the heat content of the surrounding seas on the LFR over the Indian region during the period 1996–2013. Figure 4a–d shows the seasonal mean of heat content from surface to 100 m depth over the north Indian Ocean and Fig. 4e shows the monthly climatology of heat content in the Arabian Sea (Fig. 4e, black line) and Bay of Bengal (Fig. 4e, red line) calculated using data from 1996 to 2013. Heat content over the north Indian Ocean shows maximum value during pre-monsoon with more pronounced heat over the Arabian Sea (Fig. 4a).

The seasonal variation of heat content over the Arabian Sea is seen to be decreasing with the onset of monsoon (Fig. 4b) due to cooling by strong south-westerlies, which further decreases during the post-monsoon (Fig. 4c). During winter, the heat content is again observed to be increasing over the Arabian Sea (Fig. 4d). The Bay of Bengal shows maximum heat content during the pre-monsoon season. The monthly variation of heat content shows its highest amplitude of 1.232×10^{11} Jm^{-2} during May, after which it seems to be decreasing for both the Arabian Sea (Fig. 4e, black line) and the Bay of Bengal (Fig. 4e, red line).

This maximum heat content over the Arabian Sea and Bay of Bengal during the pre-monsoon season is seen to be in line with the maximum LFR, CAPE and turbulent heat fluxes over ER and SR during the same period (Figs. 2 and 3a–b). The increase in heat content may lead to an increase in the air–sea fluxes and moisture over the sea, which then advects to the land region through the wind. LFR (Fig. 2, blue line) and turbulent fluxes (Fig. 3c, red line) over NR show maxima during June–July, whereas CAPE shows maxima during July–August (Fig. 3c, black line) compared to the heat content maxima of Arabian Sea and Bay of Bengal during May (Fig. 4e). This lag in the maxima may be due to the time taken for the influence of the heat and moisture from the seas.

To obtain a clear picture of the role of the north Indian Ocean on convection over the Indian region, the moisture advection at 850 hPa has been analysed using the data from 1996 to 2013. Seasonal mean of the moisture advection and wind vector at 850 hPa show the moisture flux propagation due to the wind forcing (Fig. 5). During pre-monsoon, the moisture advection of $\sim 0.1 \times 10^{-4}$ gkg^{-1} s^{-1} is seen from the Arabian Sea into the Indian land region. The maximum moisture flow can be observed over the western coast, the central and eastern sides of the Indian region (Fig. 5a). Most prominent moisture advection is observed during monsoon, along with the southwesterly winds over the Arabian Sea into the Indian land mass (Fig. 5b). Maximum moisture accumulation is seen along the coastal side of the Western Ghats. Moisture advection is seen to be reduced during post-monsoon and winter (Fig. 5c and d). During the winter season, moisture advection from the Bay of Bengal is observed along with the northeasterlies over the east coast of peninsular India.

These results imply the importance of heat content and moisture advection of the surrounding sea over the Indian local convective conditions. Heat content causes an increase in the air–sea fluxes over the sea. The moisture over the Arabian Sea gets advected into the Indian land region, increasing the moisture content over the boundary

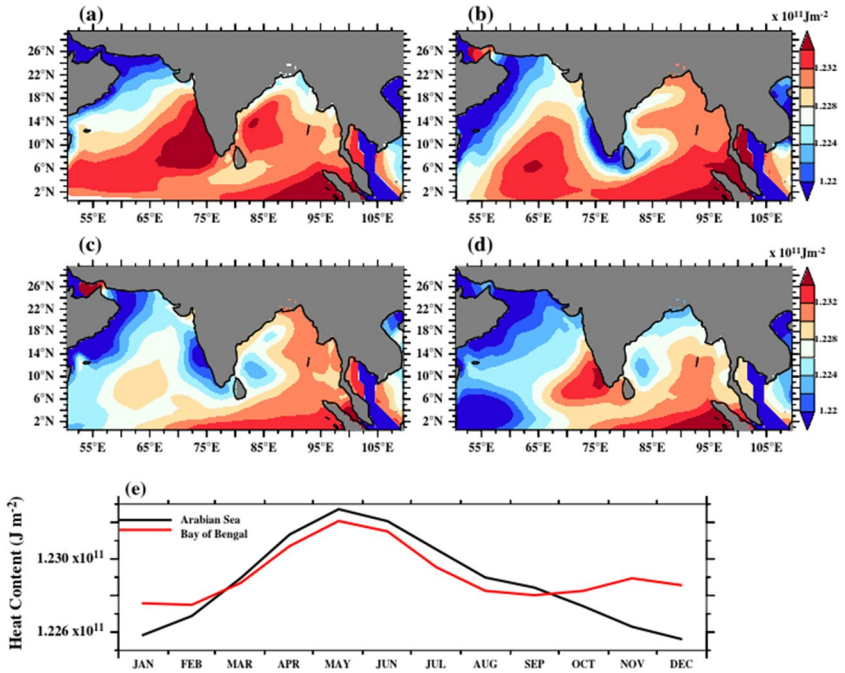

Fig. 4 Seasonal mean of heat content down to 100 m during **a** pre-monsoon, **b** monsoon, **c** post-monsoon, **d** winter and **e** monthly climatology of heat content in Arabian Sea (black line) and Bay of Bengal (red line) during 1996 to 2013

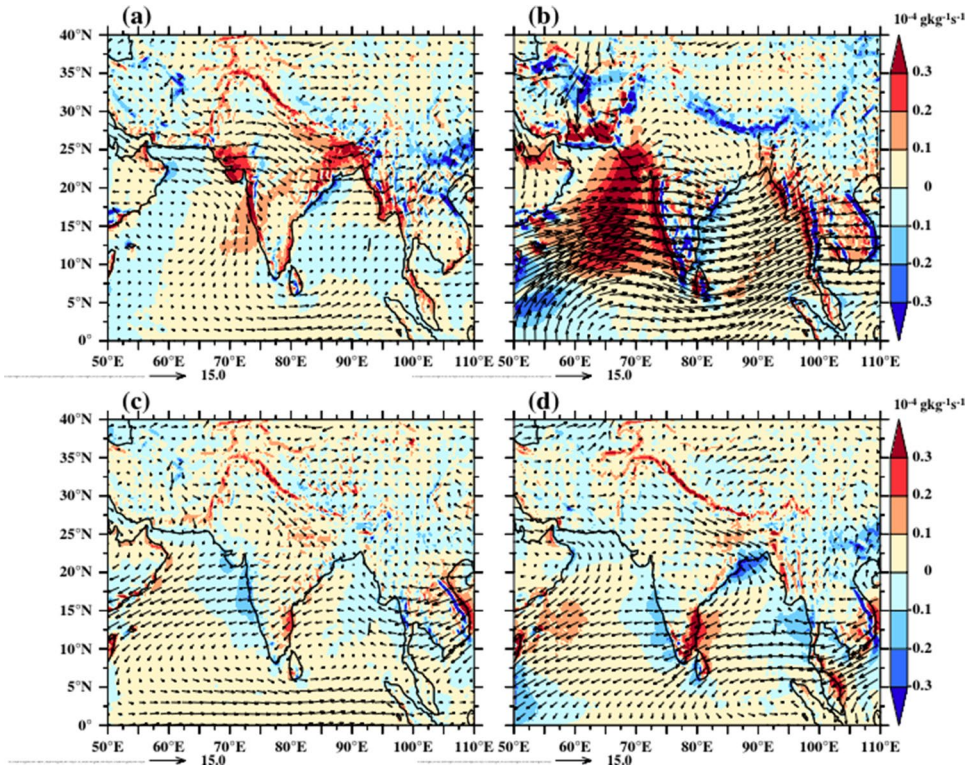

Fig. 5 Seasonal mean of moisture advection with overlaid mean wind vectors at 850 hPa during **a** pre-monsoon, **b** monsoon, **c** post-monsoon and **d** winter during 1996 to 2013

layer. These results are further analysed in detail using regression and correlation analyses in the next sections.

3.3 Multiple regression analysis of heat content and moisture advection with LFR

Table 1 shows the multiple regression analysis using monthly data of heat content and moisture advection at 850 hPa over the Arabian Sea and Bay of Bengal as independent parameters and LFR over ER, SR and NR as dependent parameters from 1996 to 2013. Regression coefficients 'b' indicates the extent of variability of the dependent variable with an independent variable when all the other independent variables are held constant. From Table 1, we can observe that for a unit change in heat content over the Arabian Sea and Bay of Bengal, LFR over ER change by 1.186×10^{-10} and 5.199×10^{-11} units, respectively. This shows a greater influence of Arabian Sea heat content over flash rates of the region compared to that of the Bay of Bengal. Similarly, for a unit change in moisture advection over the Arabian Sea

Table 1 Multiple regression analysis of heat content and moisture advection of Arabian Sea and Bay of Bengal with ER, SR and NR LFR

		Heat content (Arabian Sea)	Heat content (Bay of Bengal)	Moisture advection (Arabian Sea)	Moisture advection (Bay of Bengal)
ER LFR	*b*	1.186×10^{-10}	5.199×10^{-11}	492.3	1774.4
	b-std	0.788	0.276	0.111	0.184
	t-value	18.57	5.75	2.05	3.21
	p	< 0.0001	< 0.0001	0.04	0.001
SR LFR	*b*	3.941×10^{-11}	2.067×10^{-11}	458.1	157.1
	b-std	0.705	0.296	0.277	0.044
	t-value	14.53	5.38	4.48	0.67
	p	< 0.0001	< 0.0001	< 0.0001	0.5
NR LFR	*b*	6.175×10^{-11}	2.507×10^{-11}	− 1551.8	− 2740.6
	b-std	0.397	0.129	− 0.337	− 0.275
	t-value	10.63	3.05	− 7.09	− 5.45
	p	< 0.0001	0.003	< 0.0001	< 0.0001

and Bay of Bengal, the flash rate over ER changes by 492.3 and 1774.4 units, respectively. This shows a greater influence of moisture advection from the Bay of Bengal on the flash rate of the ER region compared to that of the Arabian Sea. The standardised regression coefficients '*b-std*' demonstrates which of the independent variables has a greater effect on the dependent variable. The heat content over the Arabian Sea (0.788) has more weightage compared to that of the Bay of Bengal (0.276), whereas the moisture advection from the Bay of Bengal (0.184) is seen to be more influential than that of the Arabian Sea (0.111) in this region (Table 1). All the values obtained are significant with $p < 0.05$ (95% confidence level).

LFR over SR change by $3.941 \times 10^{-11}$and 2.067×10^{-11} units for a unit change in heat content over the Arabian Sea and Bay of Bengal, respectively (Table 1). This shows a greater influence of Arabian Sea heat content over the LFR of the SR region compared to that of the Bay of Bengal. Similarly, for a unit change in moisture advection over the Arabian Sea and Bay of Bengal, the flash rate over SR changes by 458.1 and 157.1 units, respectively (Table 1). This shows a greater influence of moisture advection from the Arabian Sea on the LFR of the SR region compared to that of the Bay of Bengal. The standardised regression coefficients prove that the heat content and moisture advection over the Arabian Sea (0.705; 0.277) is having more weightage compared to that of the Bay of Bengal (0.296; 0.044) in this region (Table 1). The 't statistics' also confirms the above result. All the values obtained are significant with $p < 0.05$ (95% confidence level) except for the Bay of Bengal moisture advection with $p = 0.5$. The results show the impact of the fluxes through advection and low pressure systems from the surrounding seas, on the lightning parameter of the South India. This indicates the role of tropical and near-equatorial lower tropospheric weather systems (Unnikrishnan et al. 2021).

Over the NR region, LFR change by 6.175×10^{-11} and 2.507×10^{-11} units for a unit change in heat content over the Arabian Sea and Bay of Bengal, respectively (Table 1). For a unit change in moisture advection over the Arabian Sea and Bay of Bengal, flash rate over NR changed by − 1551.8 and − 2740.6 units, respectively. The standardised regression coefficients prove that the heat content over the Arabian Sea (0.397) is having more weightage compared to that of the Bay of Bengal (0.129) in this region (Table 1). The negative sign shows the effect of the cool moisture-laden monsoon current through the Himalayan foothills and plains of central India winds reducing the thermal heating and hence the lightning activity after July over the region.

The standard coefficients are less compared to the other regions from which it is evident that the heat content and moisture advection from the north Indian Ocean has less influence on the LFR over the NR region compared to the ER and SR region. NR region is characterised by dry surroundings with elevated orographic features. The thunderclouds over this region are developed under conditions with high surface temperatures and less relative humidity. Such continental areas are characterised by high Bowen ratio and less relative humidity with systematically higher cloud base (Williams and Stanfill 2002). The LFR decreases after the monsoon sets in as the cool moisture-laden winds from Bay of Bengal reaches the NR region, reducing the thermal heating over there (Kodama et al. 2005). The 't statistics' also confirm the above results. All values obtained are significant with $p < 0.05$ (95% confidence level).

Hence, the results show that the Arabian sea heat content has more influence on the variability of LFR over ER and SR regions. The moisture advection from the Arabian Sea impacts the LFR over SR, whereas it is from the Bay of Bengal over ER region. LFR over the NR region shows less dependency on the heat content and moisture advection from the north Indian Ocean compared to ER and SR.

3.4 Interannual variability of LFR and heat content

Furthermore, interannual variability of LFR and its relation with heat content in the Arabian Sea and Bay of Bengal during 1996 to 2013 is assessed in this section. Figure 6 depicts the monthly time series of LFR anomaly over ER (Fig. 6a), SR (Fig. 6b) and NR (Fig. 6c) regions from 1996 to 2013. LFR shows an increasing trend throughout the period of study for ER (slope = 5.50×10^{-5}, $p < 0.001$), SR (slope = 3.51×10^{-5}, $p < 0.001$) and NR (slope = 8.58×10^{-5}, $p < 0.001$). The values are significant above 95% confidence level. The interannual variability is more for ER and NR compared to that for SR, and hence the rate of increase of LFR is more for ER and NR.

Global and regional heat content changes serve as a robust indicator of climate change. Increased heat content increases the lifetime and intensity of the storm which in turn can lead to increased rainfall. This heat is then redistributed in the different ocean basins (Wang et al. 2018). Intergovernmental Panel on Climate Change (IPCC) report in 2013 predicted an increase in SST (Trenberth 2007) and heat content, increasing the evaporation over oceans (Trenberth et al. 2007) and providing thermal energy to the monsoon system (Sharma and Ali 2014). Thus, we have attempted to investigate the influence of heat content of the north Indian Ocean on the thunderstorm activity of the land region surrounded by the ocean. The interannual variability of heat content over the Arabian Sea and Bay of Bengal is shown in Fig. 7. Significant increasing trends are observed for heat content in the Arabian Sea (slope = 6.56×10^5, $p < 0.0001$; Fig. 7, black line) and Bay of Bengal (slope = 9.13×10^5, $p < 0.0001$; Fig. 7, red line) from 1996 to 2013, though the Bay of Bengal shows slightly higher rate of increase compared to the Arabian Sea. An opposite pattern in the heat content curve is also observed for the Arabian Sea and Bay of Bengal until 2008. Thus, this increasing

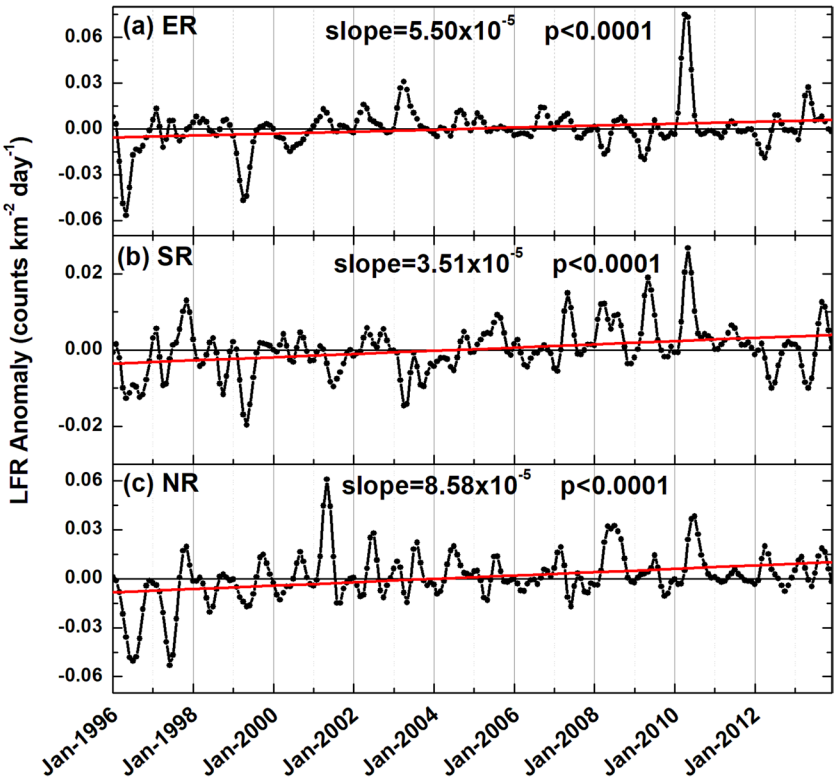

Fig. 6 Time series of monthly LFR anomaly (black line) with its trend line (red line) and slope for **a** ER, **b** SR and **c** NR from 1996 to 2013. 'p' value shows the significance of the trend line

heat content increases the heat fluxes over the sea, which gets carried into the land region, enhancing the moisture fluxes over the land. The impact of this increasing heat content on the LFR over the land region can be assessed using correlation analysis between the parameters.

To analyse the one-to-one relation, the temporal correlation between these parameters is computed and the dependency of the LFR on the heat content of the Arabian Sea and Bay of Bengal are demonstrated. Figure 8 depicts the correlation between LFR and CAPE over ER region with the heat content in the Arabian Sea (Fig. 8a and c) and Bay of Bengal (Fig. 8b and d) from surface to 100 m. LFR over ER shows a significant positive correlation ($r=0.78$; $p<0.0001$) with Arabian Sea heat content indicating that LFR over ER

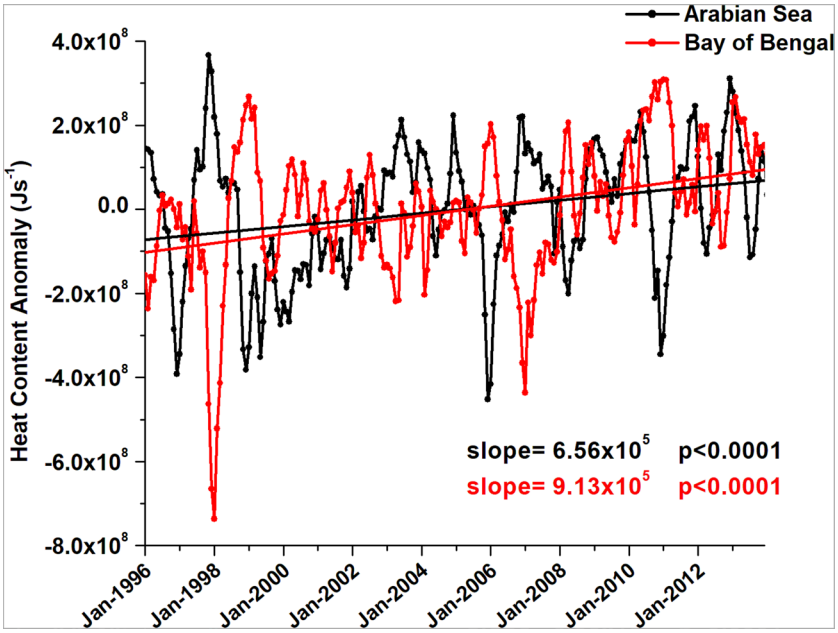

Fig. 7 Monthly time series of heat content anomaly down to 100 m with its trend line and slope for Arabian Sea (black line) and Bay of Bengal (red line) from 1996 to 2013. 'p' value shows the significance of the trend line

and Arabian Sea heat content are strongly related during the period of study. In addition, the heat content over the Arabian Sea also shows a significant positive correlation ($r=0.78$; $p<0.0001$) with CAPE over the ER region. Bay of Bengal heat content, however, shows a reduced but significant positive correlation with LFR ($r=0.41$; $p<0.0001$ and CAPE ($r=0.50$; $p<0.0001$) of ER region. These results show that an increase in the heat content of the Arabian Sea and Bay of Bengal play an important role in the development of thunderstorms over ER region, thus increasing the LFR.

Figure 9 shows the correlation analysis of Arabian Sea heat content with LFR (Fig. 9a) and CAPE (Fig. 9c), Bay of Bengal heat content with LFR (Fig. 9b) and CAPE (Fig. 9d) of the SR region. SR region shows a significant positive correlation ($r=0.69$; $p<0.0001$) with Arabian Sea heat content implying a strong relation between the parameters. Moreover, the heat content over the Arabian Sea also shows a significant positive correlation ($r=0.72$; $p<0.0001$) with CAPE over the SR region. Bay of Bengal heat content shows a significant positive correlation with LFR ($r=0.42$; $p<0.0001$ and CAPE ($r=0.43$; $p<0.0001$) of SR region. These results show the prominent influence of heat content in the Arabian Sea on the LFR over SR, though heat content in the Bay of Bengal also shows positive correlations with the LFR. This may also be due to the occurrence of more cyclonic activity in the Arabian Sea and Bay of Bengal, which are triggered by the increasing heat content. Upper ocean heat content is now considered an important parameter for the development and intensification of tropical cyclones (Mainelli et al. 2008; Pun et al. 2013; Trenberth et al. 2018) which are identified as the driving factors for the formation of thunderstorms and lightning activity over the coastal and adjoining regions (Tinmaker et al. 2010a, b).

Significant positive correlations are observed between LFR over NR region and heat content of Arabian Sea ($r=0.65$; Fig. 10a) and Bay of Bengal ($r=0.51$; Fig. 10b). However, the heat content shows less correlation with CAPE of the NR region (Fig. 10c and d). This may be due to lag between the CAPE and LFR over this region showing less correlation over the elevated regions like NR (Kamra and Ramesh Kumar 2021). The correlation values show the influence of the Arabian Sea and Bay of Bengal parameters on the development of thunderstorms over the NR region. The lightning activity in the northwest regions of Indian land increases as the surface temperature and CAPE increase. The heat low present during the starting of monsoon combined with the orographic features of the elevated regions in NR, aids for the development and outbreak of thunderstorms (Penki and Kamra 2013). As the cool Bay of Bengal branch of the monsoon current progresses to the northwest of India through the Himalayan foothills and plains of central India, the moisture-laden winds reduce the thermal heating and hence decrease the lightning activity thereafter over the region.

4 Discussion

Monthly, seasonal and interannual variations in LFR over Indian land region are studied during 1996–2013. During pre-monsoon, highest LFR is observed in NR, ER and SR

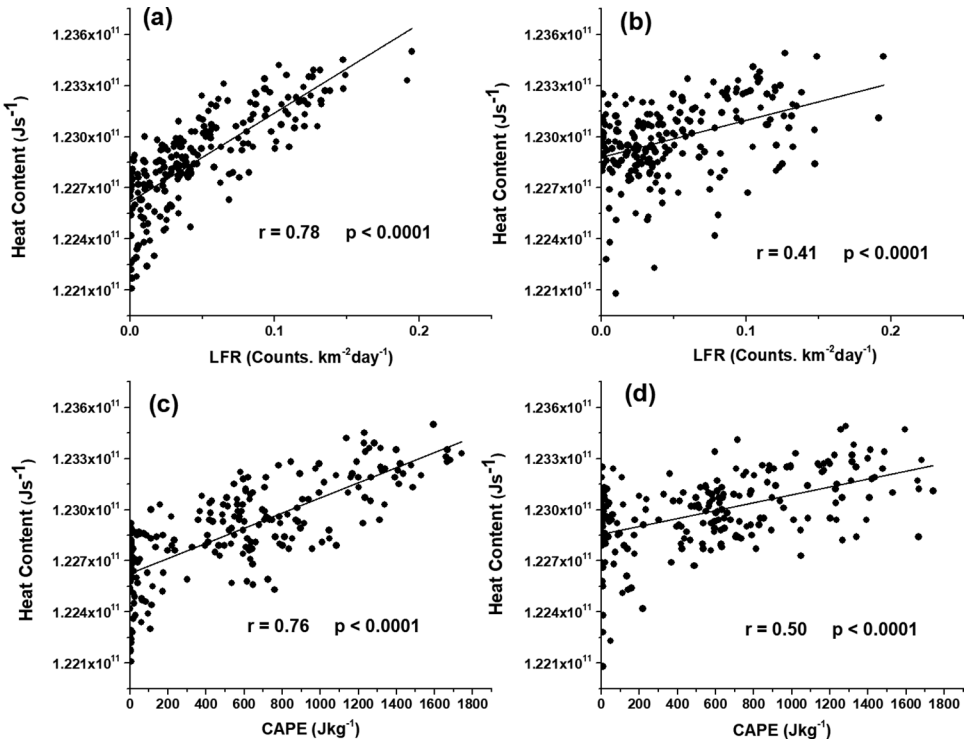

Fig. 8 Temporal correlations between **a** Arabian Sea heat content vs. ER LFR, **b** Bay of Bengal heat content vs. ER LFR, **c** Arabian Sea heat content vs. ER CAPE and **d** Bay of Bengal heat content vs. ER CAPE during 1996 to 2013. 'p' value shows the significance of the correlation

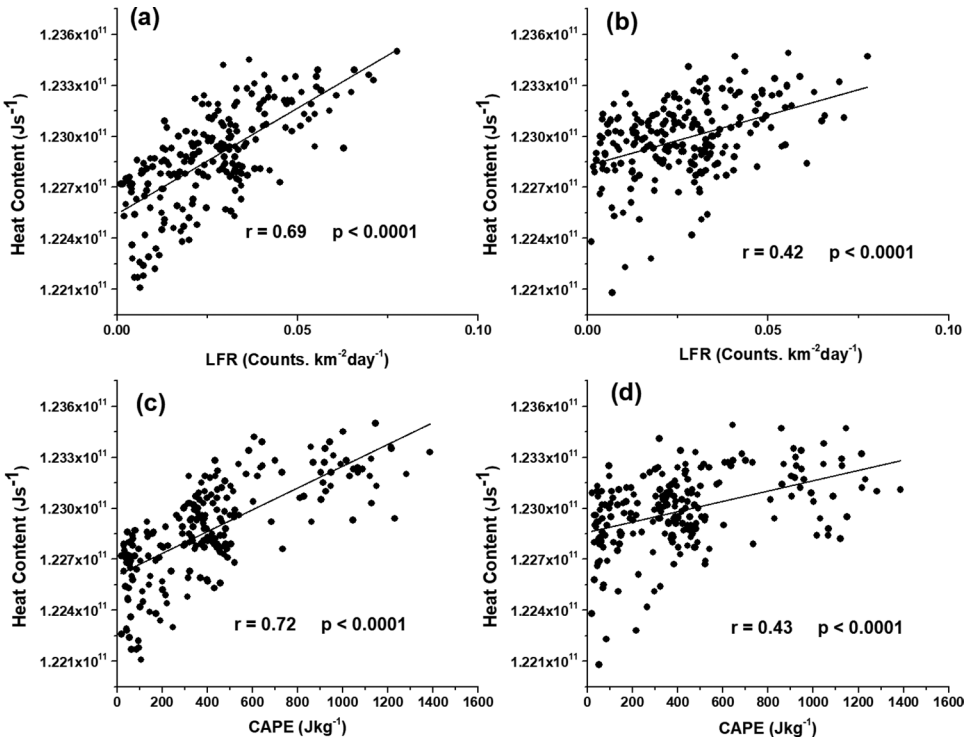

Fig. 9 Temporal correlations between **a** Arabian Sea heat content vs. SR LFR, **b** Bay of Bengal heat content vs. SR LFR, **c** Arabian Sea heat content vs. SR CAPE and **d** Bay of Bengal heat content vs. SR CAPE during 1996 to 2013. 'p' value shows the significance of the correlation

regions. Monsoon shows high LFR over NR and ER regions whereas, post-monsoon shows high LFR over NR. Less lightning activity is observed during winter over the Indian land region. Monthly climatology of LFR over ER and SR show the values peaking twice in a year during April–May and then during September–October. ER region is known for the severe thunderstorm conditions during pre-monsoon period known as Nor'wester's. During this season of the year, high solar heating of land mass causes intense convection, which then gets mixed with warm moist air from Bay of Bengal increasing

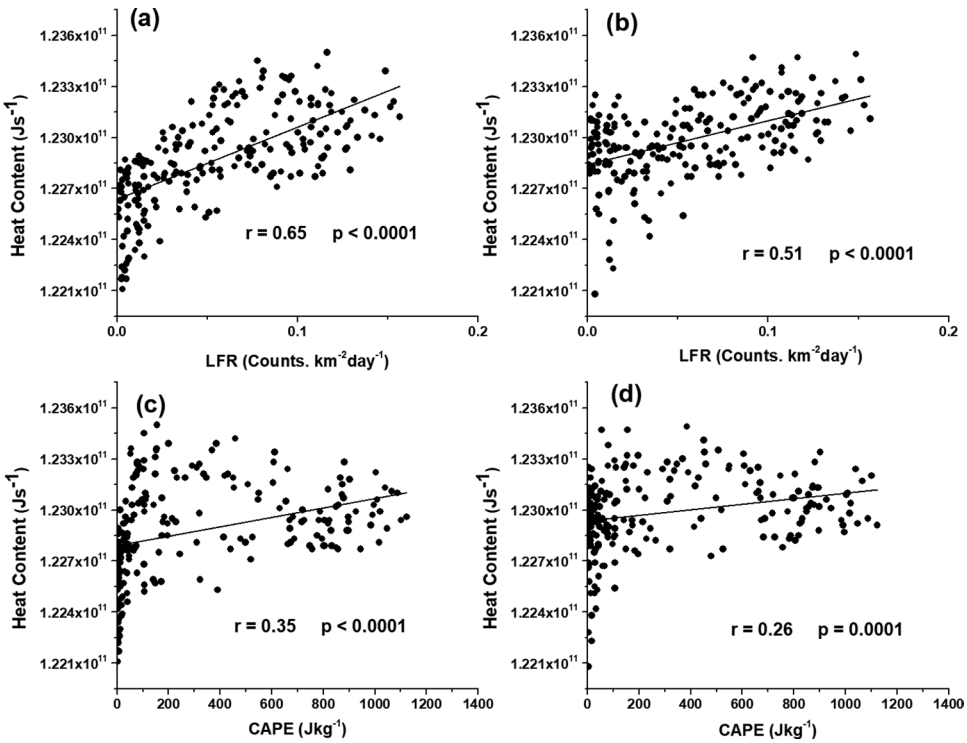

Fig. 10 Temporal correlations between **a** Arabian Sea heat content vs. NR LFR, **b** Bay of Bengal heat content vs. NR LFR, **c** Arabian Sea heat content vs. NR CAPE and **d** Bay of Bengal heat content vs. NR CAPE during 1996 to 2013. 'p' value shows the significance of the correlation

the CAPE (Penki and Kamra 2013). Pre-monsoon CAPE shows the highest value over ER (~ 1400 Jkg^{-1}). This favours the outbreak of thunderstorm over the region. The formation of greater number of low pressure systems over Arabian Sea and Bay of Bengal during the pre-monsoon period and withdrawal phase of monsoon, enhances the thunderstorms over the coastal regions like ER and SR. This explains the two peaks observed in LFR over these regions. LFR over NR shows a single maxima during June–July with rapid decrease after August. The semi-permanent heat low during May–June aids for the development of thunderstorms over the region. The orographic features with elevated terrains and high surface temperatures enhances the updraft, which justifies the increased LFR during monsoon period over NR. Regions with high altitudes and steep orographic gradient favours the formation of deep convective systems, and hence the high flash rates observed (Goswami et al. 2010; Kamra and Nair 2015). The thunderclouds over NR develop in an environment with low relative humidity, and hence are dry with low moisture content. The rainfall from these clouds gets evaporated before reaching ground because of the high cloud base and less moisture (Penki and Kamra 2013). After the arrival of monsoon, cool moisture-laden winds suppress convection with moderate updraft, thereby decreasing the LFR. The delay in arrival of monsoon winds over NR, causes the turbulent fluxes and LFR to reach its peak until July. The monthly flash rates showing annual variability for high elevated regions and semi-annual variability in all other non-elevated regions are in line with the results obtained by Kamra and Ramesh Kumar (2021).

The heat and moisture transport from Arabian Sea on the west and Bay of Bengal on the east of Indian peninsular region, gets convected into the land region, therefore increasing the air–sea fluxes, which in turn contributes to the LFR over land region. The tropical and near equatorial lower tropospheric weather systems contribute for the lighting activity over the land region (Unnikrishnan et al. 2021). Tinmaker et al. (2010a, b) have showed the crucial role of SST of the Arabian Sea and Bay of Bengal in the development of thunderstorms and lightning over the adjoining peninsular region of India. Our results show that the Arabian sea heat content has a major impact on the variability of LFR over ER and SR regions. LFR over SR are influenced by the moisture advection from the Arabian Sea, whereas over the ER region, LFR variability depends more on the moisture advection from the Bay of Bengal. Moisture advection from the north Indian Ocean have less influence on the LFR over the NR as compared to ER and SR regions. This explains the dry and less moisture-laden clouds with high cloud base over NR region.

High interannual variability and a significant increasing trend is observed in LFR from 1996 to 2013 over NR and ER region. The trend and interannual variability of heat content in Arabian Sea and Bay of Bengal also shows a significant increase throughout the period of study. The influence of warm temperature anomalies at shorter timescales over the Indian Ocean are observed on regional and global climate (Murtugudde, R., Annamalai 2004; Schott et al. 2009; Han et al. 2014). The intensification of Indian Ocean tropical cyclones was also linked to increasing Indian Ocean SST (Rao et al. 2008; Krishna 2009; Evan et al. 2011; Wang et al. 2012) and heat content (Vidya et al. 2021), which in turn cause an increase in the thunderstorm conditions over coastal land mass.

5 Conclusion

LFR over the Indian land region is analysed over different time scales and areas of higher lightning activity are identified as ER, SR and NR regions during 1996 to 2013. The causative mechanisms for such higher LFR over these regions are also investigated. ER and SR show semi-annual variability, whereas NR shows annual variability in LFR. Other than the influence of local heating, CAPE and turbulent heat fluxes, the present study brings out the significance of heat content and moisture advection from the surrounding seas on the formation of thunderstorms. An increase in the heat content of the Arabian Sea and Bay of Bengal causes enhanced moisture over the sea which gets advected to the Indian land region through the winds during the pre-monsoon and monsoon period, thereby increasing the moisture content over the land. This increase in moisture creates variations in turbulent heat fluxes over the land region, thereby increasing the intensity of thunderstorms and hence the flash rate.

The interannual variability and trend analysis of heat content shows a significant increase of heat content in Arabian Sea and Bay of Bengal. This increasing trend is also observed on LFR over ER SR and NR, with ER and NR showing the highest rate of increase. The effect of increasing heat content can be seen on global as well as regional climate variabilities. The multiple regression and correlation analyses show significant effect of heat content from the Arabian Sea and Bay of Bengal on all the major regions of high LFR. The analyses also show major impact of the moisture advection from the Arabian Sea on LFR over SR, whereas moisture advection from the Bay of Bengal have greater influence on the LFR over ER region. LFR of NR region showed less influence of the moisture advection from the seas. The thunderstorms over this region are developed under dry conditions with less rainfall.

The crucial outcome of this study is showing the importance of the surrounding ocean fluxes even on the mesoscale weather phenomenon over the land. This connection between moisture from the sea and turbulent heat flux over the land provides an insight into the coupling between ocean and atmosphere. This analysis can help provide useful information for future studies related to high thunderstorm activity. Our study is an effort in illustrating the role

of heat content on the LFR over the land region. Coupled model experiments will be needed to explore in-depth the role of the north Indian Ocean variability on the thunderstorm activity over the land.

Acknowledgements The authors would like to extend their thanks to the Department of Physics, B.M.S. College of Engineering for the facilities and support provided. The author(s) wish to acknowledge the use of the Ferret program for analysis and graphics in this paper. Ferret is a product of NOAA's Pacific Marine Environmental Laboratory. The authors also acknowledge all the freely available data used in this study, available from the links given in the data and methods section.

Author contribution All authors contributed to the study conception and design. Data analysis was performed by P.G. Nisha. The first draft of the manuscript was written by P.G. Nisha and all authors commented and provided inputs on previous versions of the manuscript. All authors read and approved the final manuscript.

Funding This work was supported by Department of Science and Technology Women Scientist Scheme (WOS-A) under grant no. SR/WOS-A/EA-18/2019, Government of India. Author P.G. Nisha has received research support from the Department of Science and Technology.

Data availability Low-Resolution Monthly Time Series (LRMTS) lightning data from January 1996 to December 2013 of 2.5° × 2.5° resolutions are retrieved from https://ghrc.nsstc.nasa.gov/lightning/data/data_lis_otd-climatology.html.

The turbulent heat fluxes like LHF and SHF, humidity, wind, and CAPE, required for the study are used from ECMWF Re-Analysis 5 (ERA5) and are available at https://www.ecmwf.int/en/forecasts/datasets/reanalysis-datasets/era5.

The monthly mean of ocean temperature and salinity data used in the study are obtained from ECMWF Ocean Reanalysis System 4 (ORAS4) and are available at.http://www.ecmwf.int/products/forecasts/d/charts/oras4/reanalysis/ from 1958 to 2017.

Code availability The codes used for all the analyses are freely available on request to the corresponding author.

Declarations

Ethics approval Not applicable.

Consent to participate Not applicable.

Consent for publication All authors agreed with the content and that all gave explicit consent to submit and we obtained consent from the responsible authorities at the institute/organisation where the work has been carried out, before the work is submitted.

Competing interests The authors declare no competing interests.

References

Balmaseda MA, Mogensen K, Weaver AT (2013) Evaluation of the ECMWF ocean reanalysis system ORAS4. Q J R Meteorol Soc 139:1132–1161. https://doi.org/10.1002/qj.2063

Cecil DJ, Buechler DE, Blakeslee RJ (2014) Gridded lightning climatology from TRMM-LIS and OTD : dataset description. Atmos Res 135–136:404–414. https://doi.org/10.1016/j.atmosres.2012.06.028

Chate DM, Tinmaker MIR, Aslam MY, Ghude SD (2016) Climate indicators for lightning over sea, sea – land mixed and land-only surfaces in India. Int J Climatol 37:1672–1679. https://doi.org/10.1002/joc.4802

Emanuel K (2015) Effect of upper-ocean evolution on projected trends in tropical cyclone activity. J Clim 28:8165–8170. https://doi.org/10.1175/JCLI-D-15-0401.1

Evan AT, Kossin JP, Chung CE, Ramanathan V (2011) Arabian Sea tropical cyclones intensified by emissions of black carbon and other aerosols. Nature 479:94–97. https://doi.org/10.1038/nature10552

Gautam AS, Joshi A, Chandra S et al (2022) Relationship between lightning and aerosol optical depth over the relationship between lightning and aerosol optical Depth over the Uttarakhand Region in India : thermodynamic perspective. Urban Sci 6:70. https://doi.org/10.3390/urbansci6040070

Goswami BB, Mukhopadhyay P, Mahanta R, Goswami BN (2010) Multiscale interaction with topography and extreme rainfall events in the northeast Indian region. J Geophys Res Atmos 115:1–12. https://doi.org/10.1029/2009JD012275

Han W, Vialard J, McPhaden MJ et al (2014) Indian ocean decadal variability: a review. Bull Am Meteorol Soc 95:1679–1703. https://doi.org/10.1175/BAMS-D-13-00028.1

Hersbach H, Bell B, Berrisford P et al (2020) The ERA5 global reanalysis. Q J R Meteorol Soc 146:1999–2049. https://doi.org/10.1002/qj.3803

Kamra AK, Nair AA (2015) The impact of the Western Ghats on lightning activity on the western coast of India. Atmos Res 160:82–90. https://doi.org/10.1016/j.atmosres.2015.03.006

Kamra AK, Ramesh Kumar P (2021) Regional variability in lightning activity over South Asia. Int J Climatol 41:625–646. https://doi.org/10.1002/joc.6641

Kandalgaonkar SS, Tinmaker MIR, Kulkarni MK, Nath A (2002) Thunderstorm activity and sea surface temperature over the island stations and along the east and west coast of India. Mausam 53:245–248

Kandalgaonkar SS, Tinmaker MIR, Kulkarni JR, Nath A (2003) Diurnal variation of lightning activity over the Indian region. Geophys Res Lett 30:1–5. https://doi.org/10.1029/2003GL018005

Kandalgaonkar SS, Tinmaker MIR, Kulkarni JR et al (2005) Spatio-temporal variability of lightning activity over the Indian region. J Geophys Res D Atmos 110:1–7. https://doi.org/10.1029/2004JD005631

Kandalgaonkar SS, Tinmaker MIR, Kulkarni MK (2008) A two year observational study of lightning and rainfall activity over Pune, India. Int J Meteorol 33:39–48

Kodama YM, Ohta A, Katsumata M et al (2005) Seasonal transition of predominant precipitation type and lightning activity over tropical monsoon areas derived from TRMM observations. Geophys Res Lett 32:1–4. https://doi.org/10.1029/2005GL022986

Krishna KM (2009) Intensifying tropical cyclones over the North Indian Ocean during summer monsoon-Global warming. Glob Planet Change 65:12–16. https://doi.org/10.1016/j.gloplacha.2008.10.007

Large WG, Pond S (1982) Sensible and latent heat flux measurements over the ocean. J Phys Ocean 12:464–482

Mainelli M, DeMaria M, Shay LK, Goni G (2008) Application of oceanic heat content estimation to operational forecasting of recent Atlantic category 5 hurricanes. Weather Forecast 23:3–16. https://doi.org/10.1175/2007WAF2006111.1

Manohar G, Kandalgaonkar S (1995) Estimation of electrical changes deposited to the ground by lightening the thunderstorms at Pune. Indian J Radio Sp Phys 24:297–307

Manohar GK, Kesarkar AP (2004) Climatology of thunderstorm activity over the Indian region : II. Spatial distribution Climatology of

thunderstorm activity over the Indian region : II. Spatial Distrib Mausam 55:31–40
Manohar GK, Kandalgaonkar SS, Tinmaker MIR (1999) Thunderstorm activity over India and the Indian southwest. J Geophys Res 104:4169–4188
Mawren D, Reason CJC (2017) Variability of upper-ocean characteristics and tropical cyclones in the South West Indian Ocean. J Geophys Res Ocean 122:2012–2028. https://doi.org/10.1002/2016JC012028
Murtugudde R, Annamalai H (2004) Role of the Indian Ocean in regional climate variability. Geophys Monogr 147:213–246
Murugavel P, Pawar SD, Gopalakrishan V (2014) Climatology of lightning over Indian region and its relationship with convective available potential energy. Int J Climatol 34:3179–3187. https://doi.org/10.1002/joc.3901
Nisha PG, Muraleedharan PM, Keerthi MG et al (2012) Does sea level pressure modulate the dynamic and thermodynamic forcing in the tropical Indian Ocean? Int J Remote Sens 33:1991–2002. https://doi.org/10.1080/01431161.2011.604653
Penki RK, Kamra AK (2013) The lightning activity associated with the dry and moist convections in the Himalayan Regions. J Geophys Res Atmos 118:6246–6258. https://doi.org/10.1002/jgrd.50499
Price C (2009) Will a drier climate result in more lightning ? Atmos Res 91:479–484. https://doi.org/10.1016/j.atmosres.2008.05.016
Pun I, Lin I, Lo M (2013) Recent increase in high tropical cyclone heat potential area in the Western North Pacific Ocean. Geophys Res Lett 40:4680–4684. https://doi.org/10.1002/grl.50548
Rao VB, Ferreira CC, Franchito SH, Ramakrishna SSVS (2008) In a changing climate weakening tropical easterly jet induces more violent tropical storms over the north Indian Ocean. Geophys Res Lett 35:L15710. https://doi.org/10.1029/2008GL034729
Romatschke U, Medina S, Houze RA (2010) Regional, seasonal, and diurnal variations of extreme convection in the South Asian region. J Clim 23:419–439. https://doi.org/10.1175/2009JCLI3140.1
Saha U, Siingh D, Midya SK et al (2017) Spatio-temporal variability of lightning and convective activity over South/South-East Asia with an emphasis during El Niño and La Niña. Atmos Res 197:150–166. https://doi.org/10.1016/j.atmosres.2017.07.005
Sarkar R, Mukhopadhyay P, Bechtold P et al (2022) Evaluation of ECMWF lightning flash forecast over Indian subcontinent during MAM 2020. Atmosphere (Basel) 13:1520. https://doi.org/10.3390/atmos13091520
Sátori G, Williams E, Lemperger I (2009) Variability of global lightning activity on the ENSO time scale. Atmos Res 91:500–507. https://doi.org/10.1016/j.atmosres.2008.06.014
Schott FA, Xie SP, McCreary JP (2009) Indian ocean circulation and climate variability. Rev Geophys 47:1–46. https://doi.org/10.1029/2007RG000245
Sharma N, Ali MM (2014) Importance of ocean heat content for cyclone studies. Oceanography 02:124. https://doi.org/10.4172/2332-2632.1000124
Sreenath AV, Abhilash S, Vijaykumar P (2021) Variability in lightning hazard over Indian region with respect to El Niño-Southern Oscillation (ENSO) phases. Nat Hazards Earth Syst Sci 21:2597–2609. https://doi.org/10.5194/nhess-21-2597-2021
Takahashi T (1990) Near absence of lightning in torrential rainfall producing Micronesian thunderstorms. Geophys Res Lett 17:2381–2384. https://doi.org/10.1029/GL017i013p02381
Tinmaker M, Ali K, Beig G (2010a) Relationship between lightning activity over Peninsular India and sea surface temperature. J Appl Meteorol Climatol 49:828–835. https://doi.org/10.1175/2009JAMC2199.1
Tinmaker MIR, Ali K, Pawar SD (2010b) Thunderstorm electrical parameters vis-à-vis rainfall and surface air temperatures over a tropical inland station, Pune, India. J Meteorol Soc Japan 88:915–924. https://doi.org/10.2151/jmsj.2010-603
Tinmaker MIR, Aslam MY, Chate DM (2014) Climatology of lightning activity over the Indian seas. Atmos - Ocean 52:314–320. https://doi.org/10.1080/07055900.2014.941323
Tinmaker MIR, Aslam MY, Chate DM (2015) Lightning activity and its association with rainfall and convective available potential energy over Maharashtra, India. Nat Hazards 77:293–304. https://doi.org/10.1007/s11069-015-1589-x
Tinmaker MIR, Ghude SD, Chate DM (2019) Land-sea contrasts for climatic lightning activity over Indian region. Theor Appl Climatol 138:931–940. https://doi.org/10.1007/s00704-019-02862-4
Toumi R, Qie X (2004) Seasonal variation of lightning on the Tibetan Plateau : a spring anomaly ? Geophys Res Lett 31:2–5. https://doi.org/10.1029/2003GL018930
Trenberth KE (2007) Observations: surface and atmospheric climate change. In: Solomon S et al (eds)Climate Change 2007: The Physical Science Basis— Contribution of WG 1 to the Fourth Assessment Report of the Intergovernmental Panel on Climate Change. Cambridge University Press, Cambridge, U. K. pp 235–336
Trenberth KE, Davis CA, Fasullo J (2007) Water and energy budgets of hurricanes: case studies of Ivan and Katrina. J Geophys Res Atmos 112:1–11. https://doi.org/10.1029/2006JD008303
Trenberth KE, Cheng L, Jacobs P et al (2018) Hurricane Harvey links to ocean heat content and climate change adaptation. Earth's Future 6:730–744. https://doi.org/10.1029/2018EF000825
Turman BN, Edgar BC (1982) Global lightning distributions at dawn and dusk. J Geophys Res 87:1191–1206
Tyagi A (2007) Thunderstorm climatology over Indian region. Mausam 58:189–212
Unnikrishnan CK, Pawar S, Gopalakrishnan V (2021) Satellite-observed lightning hotspots in India and lightning variability over tropical South India. Adv Sp Res. https://doi.org/10.1016/j.asr.2021.04.009
Vidya PJ, Balaji M, Mani Murali R (2021) Cyclone Hudhud-eddy induced phytoplankton bloom in the northern Bay of Bengal using a coupled model. Prog Oceanogr 197:102631. https://doi.org/10.1016/j.pocean.2021.102631
Wang B, Xu S, Wu L (2012) Intensified Arabian Sea tropical storms. Nature 489:E1–E2. https://doi.org/10.1038/489502c
Wang G, Cheng L, Abraham J, Li C (2018) Consensuses and discrepancies of basin-scale ocean heat content changes in different ocean analyses. Clim Dyn 50:2471–2487. https://doi.org/10.1007/s00382-017-3751-5
Williams ER (2005) Lightning and climate : a review. Atmos Res 76:272–287. https://doi.org/10.1016/j.atmosres.2004.11.014
Williams E, Stanfill S (2002) The physical origin of the land-ocean contrast in lightning activity. Comptes Rendus Phys 3:1277–1292. https://doi.org/10.1016/S1631-0705(02)01407-X
Williams E, Mushtak V, Rosenfeld D et al (2005) Thermodynamic conditions favorable to superlative thunderstorm updraft, mixed phase microphysics and lightning flash rate. Atmos Res 76:288–306. https://doi.org/10.1016/j.atmosres.2004.11.009
Yoshida S, Morimoto T, Ushio T, Kawasaki Z (2009) A fifth-power relationship for lightning activity from Tropical Rainfall Measuring Mission satellite observations. J Geophys Res 114:1–10. https://doi.org/10.1029/2008JD010370
Yuan T, Qie X (2005) Seasonal variation of lightning activities and related meteorological factors over the central Qinghai-Xizang Plateau. In: Acta Meteor Sinica, Technical Report 63(1):123–127

Publisher's note Springer Nature remains neutral with regard to jurisdictional claims in published maps and institutional affiliations.

Springer Nature or its licensor (e.g. a society or other partner) holds exclusive rights to this article under a publishing agreement with the author(s) or other rightsholder(s); author self-archiving of the accepted manuscript version of this article is solely governed by the terms of such publishing agreement and applicable law.